BIOCHEMISTRY
including biophysical chemistry & molecular biology

Article

pubs.acs.org/biochemistry

Long-Range Effects of Familial Hypertrophic Cardiomyopathy Mutations E180G and D175N on the Properties of Tropomyosin

Socheata Ly[†] and Sherwin S. Lehrer*[,†,‡]

[†]Cardiovascular Program, Boston Biomedical Research Institute, 64 Grove Street, Watertown, Massachusetts 02472, United States
[‡]Neurology Department, Harvard Medical School, Boston, Massachusetts 02114, United States

ABSTRACT: Cardiac α-tropomyosin (Tm) single-site mutations D175N and E180G cause familial hypertrophic cardiomyopathy (FHC). Previous studies have shown that these mutations increase both Ca^{2+} sensitivity and residual contractile activity at low Ca^{2+} concentrations, which causes incomplete relaxation during diastole resulting in hypertrophy and sarcomeric disarray. However, the molecular basis for the cause and the difference in the severity of the manifested phenotypes of disease are not known. In this work we have (1) used ATPase studies using reconstituted thin filaments in solution to show that these FHC mutants result in an increase in Ca^{2+} sensitivity and an increased residual level of ATPase, (2) shown that both FHC mutants increase the rate of cleavage at R133, ∼45 residues N-terminal to the mutations, when free and bound to actin, (3) shown that for Tm-E180G, the increase in the rate of cleavage is greater than that for D175N, and (4) shown that for E180G, cleavage also occurs at a new site 53 residues C-terminal to E180G, in parallel with cleavage at R133. The long-range decreases in dynamic stability due to these two single-site mutations suggest increases in flexibility that may weaken the ability of Tm to inhibit activity at low Ca^{2+} concentrations for D175N and to a greater degree for E180G, which may contribute to differences in the severity of FHC.

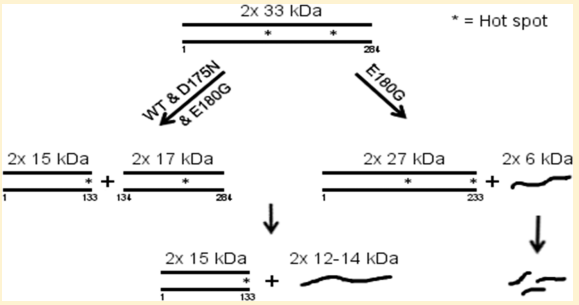

Familial hypertrophic cardiomyopathy (FHC) is a genetically transmitted disease that causes progressive remodeling of the myocardium and may result in sudden death. FHC is caused by mutations in sarcomeric proteins, including the thin filament regulatory proteins troponin (Tn) and tropomyosin (Tm).[1−3] The single-site mutations D175N and E180G in cardiac α-tropomyosin have been the subject of several studies,[4,5] including force measurements on fibers,[6,7] in vitro motility assays,[8] ATPase measurements on Tm mutants exchanged into myofibrils,[9] physiological measurements on mouse model hearts,[10] and myosin subfragment 1 (S1) binding kinetics using reconstituted thin filaments.[11] These studies suggest that incomplete relaxation of the heart at the low Ca^{2+} concentrations present during diastole coupled with the increased Ca^{2+} sensitivity can cause some of the phenotypes observed in the disease. In most cases, the Ca^{2+} sensitivity increase was greater for E180G than D175N. However, the molecular basis for the in vivo abnormal functional properties of these Tm mutants is not known.

Our early study of the properties of the D175N and E180G Tm mutants showed that (1) the binding of these mutants to actin in the absence and presence of Tn is weakened[12] (note the label mixup[13]), (2) the thermal stability of E180G is decreased, and (3) the region of the molecule near position 190 is destabilized. The strongest effects occur for the E180G FHC mutant. More recent biochemical studies have verified the weakened binding to actin.[14] These mutations are located outside of the hydrophobic region of the coiled coil but may be involved in ionic interactions across the chains.[15] Thus, the single-site mutations D175N and E180G dramatically affect the global properties of Tm, but the underlying mechanisms are not clear. It is also unknown how these effects cause the FHC phenotype.

Tm is a coiled-coil molecule stabilized primarily by hydrophobic side chain interactions between the two parallel α-helical polypeptide chains. In the actinTmTn thin filament, Tm acts in two ways: (1) by sterically inhibiting the interaction of myosin heads with actin at low Ca^{2+} concentrations and (2) by inhibiting the transition of myosin heads on actin to the force-generating state. This is the basis of the three-state model consisting of Blocked (without Ca^{2+}), Closed (Ca^{2+}-induced), and Open (myosin-induced)[16] and is correlated with three positions of Tm on actin.[17] The three-state model has provided a useful framework for understanding normal muscle regulation. Recently, we proposed the inclusion of a fourth state, an active state present in the absence of Ca^{2+} produced by strong-binding myosin heads,[18] to help understand how mutations, involving most of the sarcomeric muscle proteins, can cause cardiac diseases such as familial hypertrophic cardiomyopathy (FHC) and dilated cardiomyopathy (DCM). The FHC effects are mimicked by NEM-S1,[19] a strong binding analogue of S1 that does not dissociate from actin in the

Received: May 24, 2012
Revised: July 11, 2012
Published: July 13, 2012

   dx.doi.org/10.1021/bi3006835 | *Biochemistry* 2012, 51, 6413−6420

presence of ATP, indicating that the increase in Ca^{2+} sensitivity involves myosin.

In this work, we showed that substitution of Gly and Gln neutral amino acids with negatively charged Glu and Asp, respectively, on the outside of the Tm coiled coil affects the protein local stability ~50 residues away, a phenomenon of long-range information transfer. The decreased stability of the FHC mutants suggests a greater flexibility of Tm on the thin filament that may be important in their malfunction. The results are discussed within the framework of the four-state model recently published in which the contribution of an active state in the absence of Ca^{2+} can explain several effects produced by strong-binding myosin heads.[18]

EXPERIMENTAL PROCEDURES

Protein Preparations. The recombinant FHC Tms, WT, E180G, and D175N, were prepared from rat cardiac αTm by recombinant DNA methods as described previously.[14,20] In addition to an Ala-Ser N-terminal extension to facilitate binding to actin, a K279N mutation was included to change the rat sequence to match the rabbit and human sequences. Transfected cells were lysed using the freeze−thaw method. Buffer [50 mM Tris (pH 8.0), 1 mM EDTA, 100 mM NaCl, and 1 mM phenylmethanesulfonyl fluoride] was added to the frozen pellet, suspended, and spun to remove cell debris; the supernatant was boiled for 1 min to precipitate unwanted proteins and spun, and the supernatant was acidified to pH 4.6 to isoelectrically precipitate Tm. The resulting precipitate was dissolved in 10 mM HEPES (pH 7.5) and 100 mM NaCl and purified with a HiTrap Q column (AKTA) using a linear salt gradient from 100 mM to 1 M NaCl. Purity was confirmed by mass spectrometry and sodium dodecyl sulfate−polyacrylamide gel electrophoresis (SDS−PAGE). Protein concentrations were determined spectrophotometrically using an E_{277} (1 mg/mL) of 0.24. Actin was prepared from rabbit skeletal muscle acetone powder.[21] Myosin subfragment 1 (S1) was prepared from rabbit skeletal muscle using standard procedures.[22] Rabbit skeletal Tn was purified from ether-dried muscle powder by standard methods.[23]

Methods. Trypsin digestion was performed on Tm at 0.5 mg/mL in 10 mM HEPES buffer (pH 7.5), 0.1 M NaCl, 5 mM $MgCl_2$, and 10 mM β-mercaptoethanol, treated with 0.001 mg/mL porcine trypsin (G-Biosciences catalog no. 786-245). For digestion of actinTm, 0.003 mg/mL trypsin was mixed with 1.5 mg/mL F-actin and 0.3 mg/mL Tm (excess actin) in the same buffer solution. The reactions were quenched with a 20-fold excess of soybean trypsin inhibitor (STI) by weight with respect to trypsin. All digestions were conducted at 26 °C. Polyacrylamide handcast gels (12.5%) were used to visualize Tm digestion, and 12% Mini-Protean TGX Precast Gels (Bio-Rad catalog no. 456-1043) were used for actinTm digestion. Coomassie-stained gels were scanned and analyzed with ImageJ. The band density of Tm at time zero was used to normalize all band densities.

An Aviv 60DS CD circular dichroism spectropolarimeter was used for monitoring thermal unfolding. Tm (1 mg/mL) in buffer [10 mM HEPES (pH 7.5) and 100 mM NaCl], in a 1 mm cuvette, was incubated with 1 mM dithiothreitol (DTT) and heated to 40 °C for 15 min to reduce possible S−S bonds. The CD signal at 222 nm was recorded during temperature scans (at 1 °C/min) between 25 and 70 °C.

Mass spectrometry was performed on 1:1 protein samples with 20 mg/mL sinapinic acid in 50% CH_3CN and 0.1% TFA and analyzed with a Perceptive Voyager matrix-assisted laser desorption ionization time-of-flight (MALDI-TOF) instrument.

Tm digests were analyzed by SDS−PAGE and transferred onto an Immobilon-P^{SQ} PVDF 0.2 μm membrane (Millipore ISEQ26260). N-Terminal amino acid sequence analyses were performed by M. Berne (Tufts University, Boston, MA).

Acto-S1 ATPase activity was measured spectrophotometrically using the EnzCheck Phosphate Assay Kit (Molecular Probes). The continuous linear production of P_i with time was monitored on a Cary 50 UV−vis instrument for each addition of sample to low-salt buffer [20 mM HEPES (pH 7.5), 15 mM NaCl, 3 mM $MgCl_2$, and 1 mM DTT] containing 0.1 mM $CaCl_2$ from stock solutions in the following order: 1 mM ATP, 0.2−0.5 μM S1, 4 μM actin, 1−2 μM Tm, 1−2 μM Tn, and 1 mM ethylene glycol tetraacetic acid (EGTA) with 1 mM nitrilotriacetic acid (NTA). Monitoring the linear A_{360} versus time gave relative ATPase values for S1 background, actin activation, Tm inhibition, Tn activation with Ca^{2+}, and Tn inhibition without Ca^{2+}. For the ATPase versus Ca^{2+} concentration measurements, the samples contained 0.5 μM S1, 4 μM actin, 1 μM Tm, and 1 μM rabbit skeletal Tn. The proteins were mixed into low-salt buffer as described above with addition of 0.5 mM EGTA and 0.5 mM nitrilotriacetic acid. ATP (1 mM) and S1 background activity was obtained and subtracted from all calculations. The reaction solution was titrated with 20 mM $CaCl_2$. $[Ca^{2+}]_{free}$ was calculated using Maxchelator (http://maxchelator.stanford.edu). All ATPase experiments were conducted at room temperature (25 °C).

RESULTS

S1-Actin ATPase. ATPase measurements with reconstituted thin filaments were performed using the continuous colorimetric measurement of phosphate liberation during successive mixing in of myosin subfragment 1 (S1), actin, Tm, Tn with Ca^{2+}, and Tn without Ca^{2+} (Figure 1a; see Experimental Procedures). Tm and Tn bound fast to actin and actinTm, respectively, as evidenced by the quick linear dependence of phosphate liberation after each addition. In the absence of Tn and Ca^{2+}, WT and D175N inhibited actin-S1 activity by ~80 ± 3%, whereas E180G inhibited activity by only 64 ± 5%. Similarly, in the presence of TmTn with Ca^{2+}, the S1-actin ATPase activity was inhibited by 45 ± 1 and 47 ± 8% for WT and D175N, respectively, whereas E180G inhibited somewhat less (37 ± 7%). Finally, the S1-actinTmTn ATPase in the absence of Ca^{2+} for both WT and D175N was inhibited by 85 ± 3%, whereas the inhibition for E180G was weaker (74 ± 6%). Doubling the concentration of Tm or/and Tn did not change the results within experimental error. These data show that there is less inhibition of ATPase for E180G under all conditions.

Titrations with Ca^{2+} in an EGTA/nitrilotriacetic acid buffer system showed increased Ca^{2+} sensitivity of S1-actinTmTn ATPase for D175N and E180G indicated by the shift of the midpoint of the ATPase curves to lower Ca^{2+} concentrations. We also obtained greater residual activity at very low Ca^{2+} concentrations for E180G (Figure 1b). E180G showed the largest effect of enhanced residual ATPase in agreement with Figure 1a, and the greatest Ca^{2+} sensitivity. The Hill coefficients were 2.11 ± 0.08, 1.62 ± 0.04, and 1.89 ± 0.08 for WT, D175N, and E180G, respectively. Considering the different systems and measurements, these data obtained with reconstituted thin filaments in solution reasonably agree

dx.doi.org/10.1021/bi3006835 | Biochemistry 2012, 51, 6413−6420

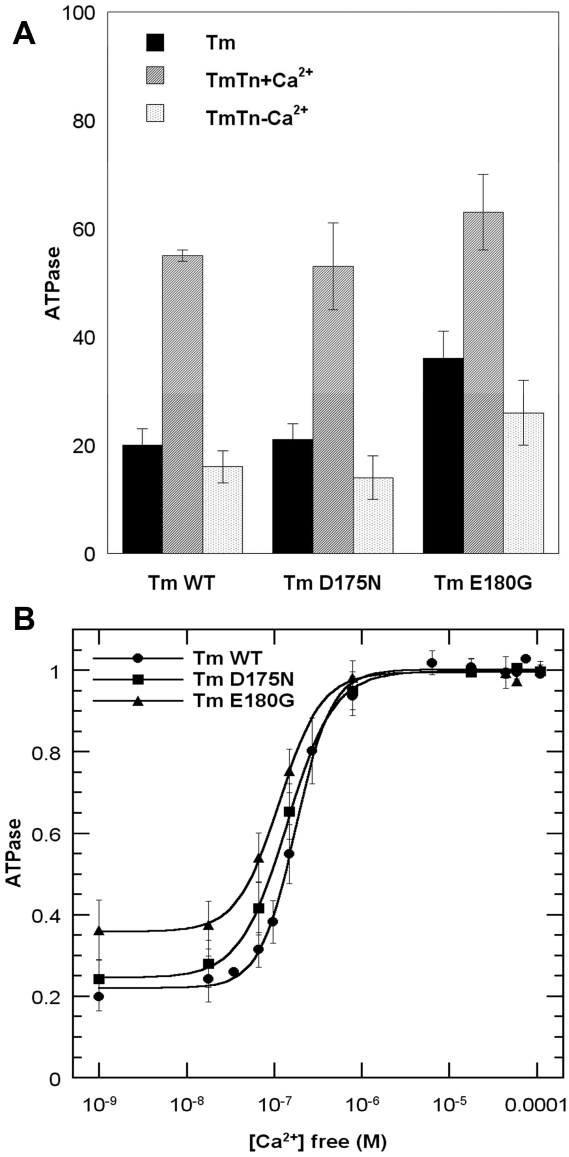

Figure 1. Effects of Tm FHC mutants on actin-S1 ATPase activity. Data obtained by continuously monitoring Pi liberation (see Experimental Procedures). (A) Effects of Tm and Tn with or without Ca^{2+}. ATPase was monitored during successive additions of S1, actin, Tm, Tn, and EGTA to a solution containing, 0.1 mM $CaCl_2$, 15 mM NaCl, 3 mM $MgCl_2$, 1 mM DTT, and 1 mM ATP in buffer [10 mM HEPES (pH 7.5)]. Data were normalized to actin-S1 activity after subtraction of the background S1 ATPase. (B) ATPase vs $[Ca^{2+}]$. $CaCl_2$ was titrated into the reconstituted actinTmTn thin filament in buffer containing 1 mM EGTA and 1 mM NTA. Data were normalized to the high Ca^{2+} concentrations fitted to the Hill equation. Background S1 alone ATPase was subtracted.

qualitatively with measurements of ATPase in fibers and with physiological experiments that measured pCa versus force.[6,7]

Thermal Unfolding. To compare the global stability of the samples, we studied the thermal unfolding transitions with circular dichroism (Figure 2). WT and D175N showed a major transition at 47 °C and a shoulder at 55 °C. E180G was markedly less stable, with the early transition shifted 5 °C to a lower temperature without an effect on the high-temperature transition. These data confirm our earlier results for different constructs of the same mutants,[12] corrected for the sample mislabeling (see ref 13 for the erratum) except for a small shift

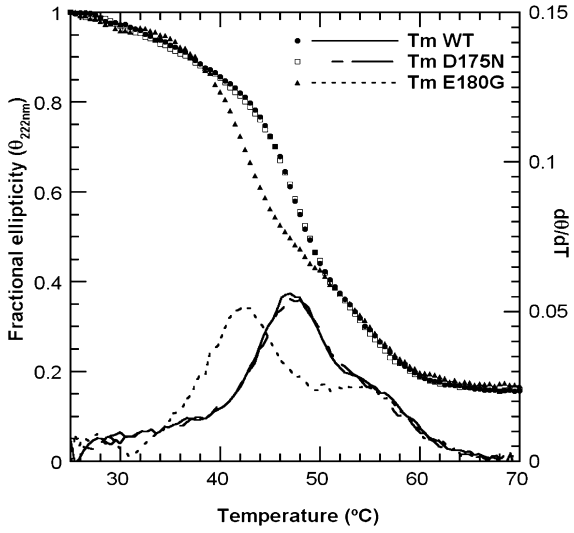

Figure 2. CD thermal unfolding profiles at 222 nm (Θ vs T) and derivatives ($d\Theta/dT$) of the Tm FHC mutants and WT control. Samples contained 1 mg/mL protein in 100 mM NaCl, 10 mM HEPES buffer (pH 7.5), and 1 mM DTT .

of the transitions to greater temperature probably because of different solution conditions. More recent studies using differential scanning calorimetry produced similar results.[14] Thus, the single-site mutant E180G destabilizes a very large part of Tm, whereas the D175N mutation has little effect on thermal stability.

Trypsin Digestion. Using the limited trypsin digestion approach with Tm,[20,25] we studied the early cleavage progress on WT, D175N, and E180G. This treatment produced a dimer of 17−18 kDa chains and a dimer of 15 kDa from the intact Tm dimer of 33 kDa seen on gels as some digits at the end (Figure 3 and Table 1). Each purified peptide was shown to be largely α-helical at room temperature.[25] In a separate CD experiment during a similar treatment of rabbit cardiac Tm with trypsin, we noted that only ~13% of the Tm helix was lost at 30 min when most of the Tm was cleaved. For all Tms, the 17−18 kDa C-terminal peptide seen in gels (34−36 kDa dimer) was further cleaved, faster than the 15 kDa peptide (30 kDa dimer), in agreement with its lower stability.[25] Cleavage of the dimer (17−18 kDa peptide) produces a 13−14 kDa peptide as seen by the lag in its appearance and the increase in its level as the level of the 18 kDa form decreases (Figure 3). A slightly lower-molecular mass species in the main Tm band (33 kDa) was observed to appear with time. This is due to simultaneous truncation of seven amino acids at the N-terminus as shown previously.[20]

N-Terminal sequencing verified that the initial cleavage site was at Arg133 (Table 1). The rate of cleavage of Tm was greater for the FHC mutants as judged by the decrease in the half-time of loss of Tm from 11 min for WT to 6 and 3 min for D175N and E180G, respectively (Figure 3). Thus, the two FHC mutations increased the rate of cleavage of a residue located ~50 residues N-terminal from the mutation site.

For E180G, the initial cleavage also took place at another site with a rate similar to the rate of cleavage at R133 as evidenced by the early appearance of a band at ~27 kDa in parallel with the appearance of the 18 kDa band (Figure 3). The site of cleavage was tentatively identified by comparing the molecular mass determined by MALDI-TOF with the calculated molecular mass of fragments cleaved at Arg or Lys in the C-

dx.doi.org/10.1021/bi3006835 | Biochemistry 2012, 51, 6413−6420

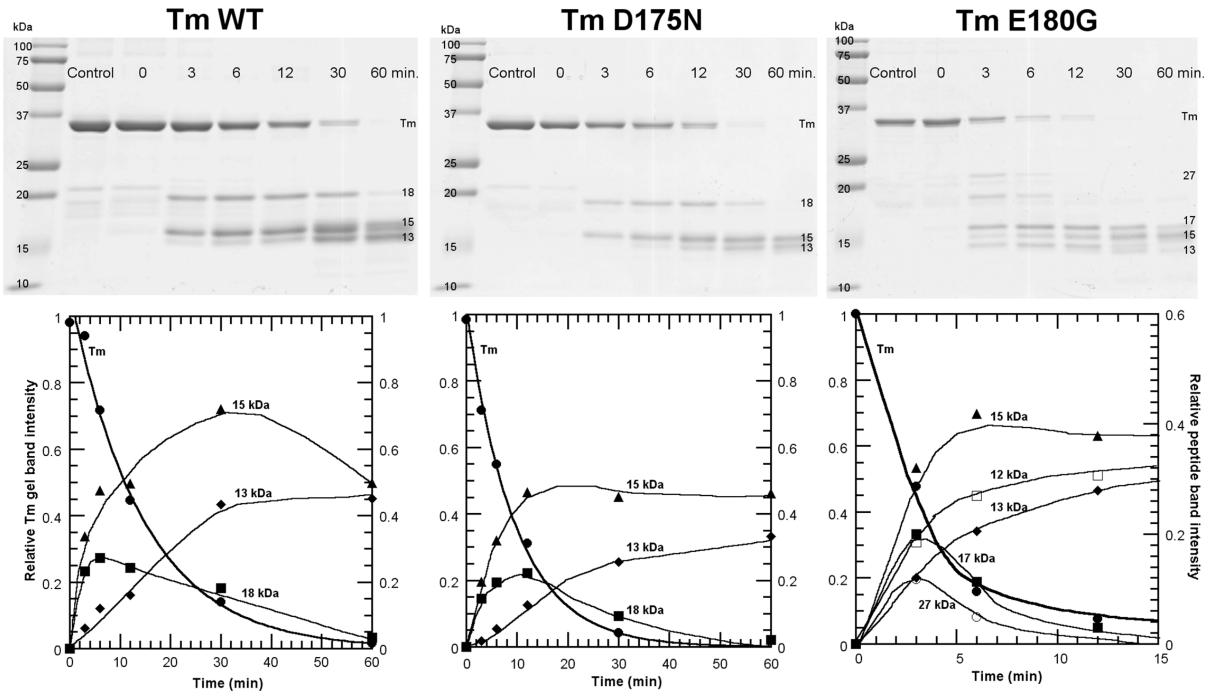

Figure 3. Kinetics of trypsin digestion of FHC Tms and WT control: (top) 12.5% polyacrylamide−SDS gels quenched at the indicated times and (bottom) densitometric analyses showing the kinetics of the change of gel bands. The densities were normalized to the density of Tm at time zero.

Table 1. Identification of Tryptic Peptides via N-Terminal Sequencing and MALDI-TOF Molecular Mass Determination[a]

	gel band (kDa)	observed molecular mass (kDa)	calculated molecular mass (kDa)	N-terminal sequence (observed)	peptide sequence
WT and D175N	18	17.66	17.568	(R) AQKDE	134−284
	15	15.37	15.289	ASMDA	1−133
	13	13.67		(R) KLVII	168−284
				(K) HIAED	153−284
				(K) MQMLK	8−133
E180G	27	26.83	[26.90]	–	[1−233]
	17	17.47	17.496	(R) AQKDE	134−284
	15	15.21	15.289	ASMDA	1−133
	13−14	13.56		(R) KLVII	168−284
				(K) MQMLK	8−133
		14.46		(R) AQKDE	[134−233]

[a]Molecular masses of Tms (including AS extension) were as follows: WT, 32839 Da; D175N, 32838 Da; E180G, 32762 Da. Brackets denote tentative sequence.

terminal region of Tm. Thus, the single-site mutation from Asp to Gly at position 180 produced another region of dynamic instability at K233, a site located 53 residues C-terminal to the mutation site.

When Tm is bound to actin, the rate of Tm cleavage was decreased 16-fold for WT, 20-fold for D175N, and ∼30-fold for E180G, correcting for the difference in trypsin concentration. A similar deceleration by actin was observed in our work with native Tm.[24] Despite the overall deceleration of cleavage, the increased rate for the FHC mutants still persisted ($t_{1/2}$ values of 60, 40, and 32 min for WT, D175N, and E180G, respectively). Evidence that Tm was cleaved when bound to actin and not cleaved when free in solution was obtained by the absence of a faster-moving Tm band on gels due to truncation of seven amino acid residues from the N-terminus (nine including the added Ala and Ser) that occurs in parallel with cleavage for free Tm and for these samples in the absence of actin.[20] This protection is probably due to Tm end-to-end interactions or shielding by actin. As noted previously,[20] the actin was not cleaved by trypsin over the 1.5 h time period. As for Tm alone, a 15 kDa gel band was present at early times, but a 17−18 kDa band and a 27 kDa band were not observed in the gels even at short times. This appears to be due to loss of binding to actin of the cleaved peptides[26] and the more rapid cleavage of the 18 and 27 kDa peptides than the 15 kDa peptide when they are free in solution, especially at a concentration 3 times the trypsin concentration (Figure 4).

N-Terminal sequencing of the blotted peptides from gels and MALDI-TOF MS allowed identification of most of the peptides (Table 1). For WT and D175N, the N-terminal half (15 kDa) and the C-terminal half (17 kDa for E180G and 18 kDa for WT and D175N) were as identified previously.[20] The 18 kDa band was degraded further to produce species between 13 and 15 kDa. N-Terminal sequencing of the broad gel band in that region showed the presence of peptides 168−284 and 153−284 and a C-terminal peptide truncated at Lys7 (peptide 8−133). For E180G, the same two initially cleaved halves at 15 and 17 kDa were identified. However, for E180G, a new gel band at 27

dx.doi.org/10.1021/bi3006835 | *Biochemistry* 2012, 51, 6413−6420

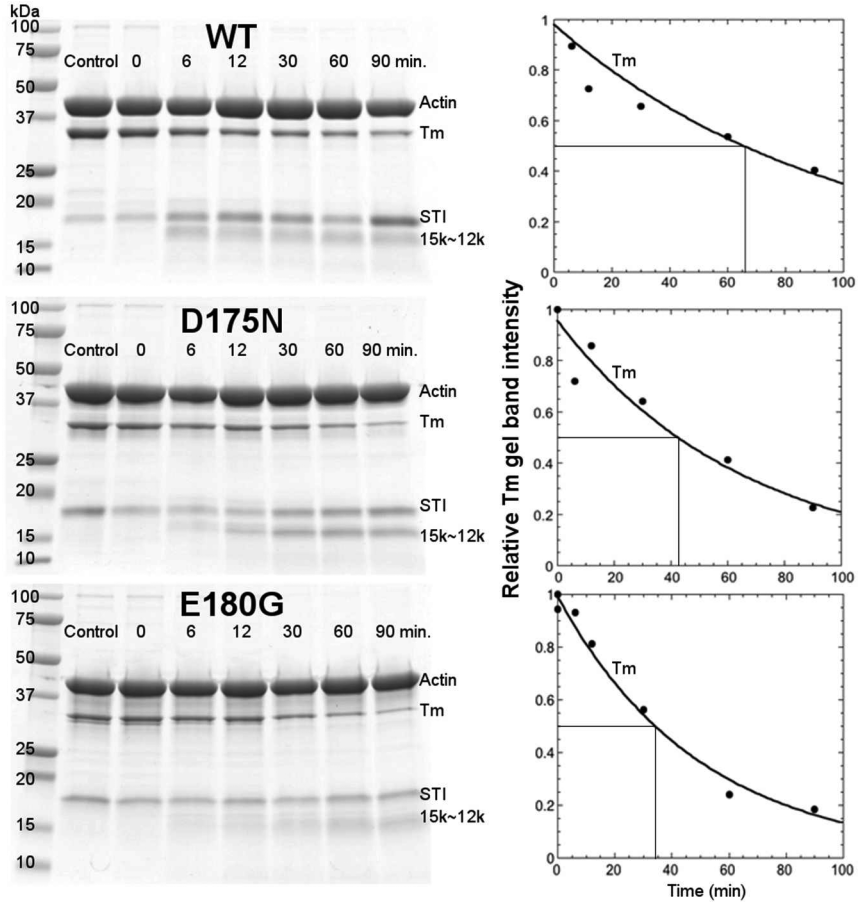

Figure 4. Kinetics of trypsin digestion of Tm FHC mutants and WT control bound to actin: (left) 12.5% polyacrylamide−SDS gels quenched at the indicated times and (right) densitometric analysis of the kinetics of cleavage of Tm normalized to time zero.

kDa (54 kDa dimer) was tentatively identified at Lys233. At longer reaction times, peptides created by further cleavage of the 27 kDa band of E180G were observed below 15 kDa. Some of these peptides from E180G corresponded to the small peptides observed for the other two Tms. An additional peptide of ~13 kDa seems to span A134−K233. It is tentatively identified as the product of the 17 kDa peptide cleaved at K233.

The pathway of cleavage for WT, D175N, and E180G is shown in Figure 5. Peptides of <15 kDa are shown as single chains because of their instability. From the results described above, it is seen that there is a "hot spot" that allows preferential cleavage at R133 for all three Tms and an additional hot spot at K233 for E180G.

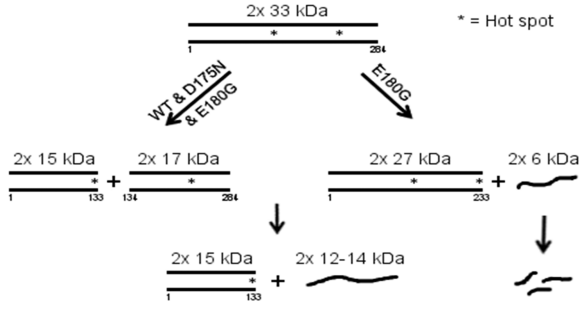

Figure 5. Schematic of the course of cleavage by trypsin. Note the common pathway for all via initial cleavage at R133 and an additional pathway for E180G with cleavage at K233. Helical peptides are indicated as dimers. Asterisks denote hot spots where cleavage occurs preferentially.

DISCUSSION

Our principal finding is that the FHC Tm mutations D175N and E180G, located about two-thirds of the distance from the N-terminus of the molecule, increase the initial rate of cleavage by trypsin at R133, located near the middle of Tm. The increase in rate was 2-fold for D175N and 4-fold for E180G. Our previous work showed that native $\alpha\alpha$Tm is initially cleaved by trypsin at R133, because of the presence of a charged Asp in the hydrophobic ridge at nearby D137, first observed by Pato et al.[25] Substitution of canonical Leu for Asp137 markedly inhibited the cleavage.[20] To cleave an α-helix by trypsin, a transient unfolding of approximately eight continuous amino acid residues of the polypeptide chain (approximately two turns of α-helix) is required,[27] which is a very small fraction of the Tm molecule. Because of the strong interchain interactions in the Tm coiled coil, both chains may unfold simultaneously. The limited tryptic digestion is therefore a test of local dynamic instability that is not observed by equilibrium measurements. The region that transiently unfolds to allow trypsin cleavage represents a hot spot in the sequence (Figure 5) that would provide flexibility around that region. A recent study also used the method of limited trypsin cleavage at R133 to study the effect of another amino acid substitution.[28]

Over the years, there have been several studies that have produced evidence of the flexibility of Tm. Early studies

dx.doi.org/10.1021/bi3006835 | *Biochemistry* 2012, 51, 6413−6420

showed that a small helix pretransition in the 35−40 °C range is associated with unfolding of approximately 10−20% of the helix in the middle of the molecule,[29−32] suggesting nonuniform stability contributing to flexibiity. This is seen in this work as a shoulder on the derivative curves (Figure 2). Fluorescence probe studies with the label at Cys190 have indicated that the probe responds to the unfolding in the pretransition temperature region.[12,13,33] The main transition at 47 °C is due to unfolding of the C-terminal region, and the transition at ∼54 °C is due to unfolding in the N-terminal region.[25,26,32] The relative areas under the derivative curves in Figure 2 can be associated with the relative size of the unfolding domains and indicate that as many as 2 times as many residues are unfolded in the C-terminal domain as in the more stable N-domain. It thus appears, for Tm, in order of stability, the unfolding domains approximately involve 20% of the residues in the middle of the molecule, 55% of the C-terminal domain, and 25% of the N-terminal domain. The unfolding transitions are cooperative, which suggests that the corresponding regions behave as independent structural domains. These domains are at odds with the seven quasi-equivalent regions identified in the amino acid sequence of Tm, which appear to act as sites of interaction with the actin monomers.[34] These regions have somewhat differing actin binding properties,[35] but no apparent correspondence between the thermal stability and the strength of the interaction with actin can be inferred. Finally, the region containing the D175N and E180G mutations is of special interest because of its presumed involvement in the interaction with troponin; e.g., preliminary data showed that a cross-link could be formed between Tm at position 176 and TnT between residues 171 and 174.[36] Thus, the mutations could affect the properties of the thin filament in several different ways.

The further decreased stability of the C-terminal domain, observed for E180G, and the dynamic unfolding revealed by limited trypsin digestion for both FHC mutants indicate flexibility that could be manifested at physiological temperature when the mutants were subjected to a perturbation such as may occur during the movement of Tm during regulation.

Recent theoretical and experimental studies involving persistence length, a measure of flexibility, produced different values ranging from 20 nm[37] to 50 nm[38] to ∼400 nm.[39] These studies assume a relatively uniform semiflexible molecule. Another measure of flexibility is the cooperative unit size, *n*, which involves the ability of strong binding myosin heads to move Tm, opening *n* actin subunits. We obtained values of ∼7−14 actin subunits uncovered by one rigor myosin head depending upon the absence or presence of Tn or the source of the Tm.[12,40,41] Other regions that may introduce flexibility have been suggested by X-ray structural studies. Regions containing several Ala residues in hydrophobic positions have been associated with bends in the coiled coil.[42] The Glu residues in the hydrophobic ridge appear to be near regions of local coiled-coil chain separation allowing penetration by water molecules.[43] Surprisingly, trypsin does not cleave in these regions.

It is difficult to understand how the E180G single-site mutation can cause the large domain instability and how both E180G and D175N single-site mutations cause the increase in long-range dynamic instability measured by the rate of trypsin cleavage, particularly in the rod-shaped Tm molecule, where interactions between nonadjacent regions are not possible. Both mutants involve the loss of a negative charge in the native Tm, located at positions e (E180) and g (D175) in the seven-residue repeat of the helix (abcdefg). These sites are involved in e−g ionic interactions across and within the chains,[15] and the loss of the favorable charge interactions could be the cause of the instability. E180G exhibits more drastic disease phenotypes, and this may be related to its greater flexibility caused by the instability. It appears that the local instability or unfolding generated in the mutation region is transmitted to the R133 region and in the case of the E180G to both the R133 and D233 regions. Recently, long-range conformational changes in two coiled coils have been proposed to involve a shift in the register of heptad repeats.[44−46] Local unfolding could be transmitted via thermal fluctuations analogous to the movement of imperfections in a crystal lattice[47] to distant unstable regions (hot spots).

It should be noted that these FHC mutations are located in a region of Tm that interacts with Tn. Fluorescent probes at position 190 are sensitive to Tn binding,[48] and more recently, a 9 Å cross-link between a Cys substituted at position 176 of Tm was found on TnT in the region of residues 171−174.[36] It is therefore possible that the interaction with Tn is perturbed due to the mutations, which could cause the increased Ca^{2+} sensitivity.

Recently, a fourth state, a substate of the three-state regulation model, has been proposed to aid in understanding FHC and other phenomena that involve activation by myosin.[18] The involvement of the fourth state can explain the increased Ca^{2+} sensitivity and increased basal activity at low Ca^{2+} concentrations. In the fourth state, Tm is in an Open or active state where it does not block myosin−nucleotide binding or the strong-binding myosin head force-generating transition, but this Open state does not have Ca^{2+} bound to TnC. In this proposed fourth state, TnI is bound to TnC after dissociation from actinTm caused by strong-binding myosin heads.[49,50] It has been shown that binding of TnI to TnC increases the affinity of Ca^{2+} for TnC-TnI.[51−53] Thus, the presence of a fourth state explains both the residual force in the absence of Ca^{2+} and the increased Ca^{2+} sensitivity. We have shown that the strong binding of two to three myosin heads per Tm was sufficient to release TnI-TnC (absence of Ca^{2+}) and TnI[49] from actinTm and TnI from actinTmTn (absence of Ca^{2+}).[50] We postulated that a TnI binding site involving both actin and Tm was lost when Tm was moved from the Blocked to the Open state by the binding of only a few heads per Tm. The increase in flexibility of the FHC Tm mutants suggested in this work could increase the contribution of the activation pathway involving the fourth state because the flexible FHC Tm mutants do not interact with the thin filament as strongly as WT, resulting in less blocking of myosin head binding, allowing more heads to enter the force-generating state via the fourth state. Weaker binding of these mutants to actin has been observed.[12,14] We also obtained here a decreased level of inhibition of ATPase in the absence of Tn (actinTm) for the E180G mutant, indicating weaker interaction. Evidence of a slightly lower level of occupation of the Blocked state for E180G was obtained from S1 binding kinetics[11] and for a stronger interaction of myosin with actin.[54] Many of the sarcomeric proteins have mutations that produce different levels of severity of FHC and DHC and show variable amounts of Ca^{2+} sensitivity and basal activity. Thus, any change in the myosin cross-bridge interaction with actin, interaction of Tm with actin as seen here, or the affinity of TnI and Ca^{2+} for TnC or TnI for actinTm, due to mutations,

dx.doi.org/10.1021/bi3006835 | *Biochemistry* 2012, 51, 6413−6420

could change the contribution of the fourth state, resulting in increases (in FHC) or decreases (in DHC) in Ca^{2+} sensitivity.

In addition to FHC, other phenomena, such as the effect of sarcomere length on Ca^{2+} affinity[55] and stretch activation of cardiac[56] and insect flight muscle,[57] also appear to be related to thin filament activation by myosin heads.

In conclusion, the work presented here, for Tm FHC mutations D180G and E175N, provides a possible link between the severity of FHC and the degree of molecular flexibility manifested as a result of the mutation. Clearly, further studies will be needed to help explain the molecular details of these long-range effects and how they are related to the severity of these myopathies.

AUTHOR INFORMATION

Corresponding Author

*Phone: (617) 658-7812. E-mail: lehrer@bbri.org.

Funding

Supported by National Institutes of Health Grant HL 91162.

Notes

The authors declare no competing financial interest.

ACKNOWLEDGMENTS

We are grateful to Dr. Zenon Grabarek for helpful suggestions during the course of the experiments and for critical reading of drafts of the manuscript. We also thank Dr. Sarah Learman, Dr. F. Timur Senguen, and Ms. Betty Gowell for experimental help and Dr. Robin Maytum (University of Bedfordshire, Luton, U.K.) for constructs and transformed cells.

ABBREVIATIONS

Tm, tropomyosin; Tn, troponin; TnI, TnC, and TnT, Tn subunits; actinTmTn, reconstituted thin filament; S1, myosin subfragment 1; FHC, familial hypertrophic cardiomyopathy; DHC, dilated hypertrophic cardiomypathy.

REFERENCES

(1) Watkins, H., Seidman, J. G., and Seidman, C. E. (1995) Familial hypertrophic cardiomyopathy: A genetic model of cardiac hypertrophy. *Hum. Mol. Genet.* No. Spec. No. 4, 1721−1727.

(2) Tardiff, J. C. (2005) Sarcomeric proteins and familial hypertrophic cardiomyopathy: Linking mutations in structural proteins to complex cardiovascular phenotypes. *Heart Failure Rev. 10*, 237−248.

(3) Redwood, C. S., Moolman-Smook, J. C., and Watkins, H. (1999) Properties of mutant contractile proteins that cause hypertrophic cardiomyopathy. *Cardiovasc. Res. 44*, 20−36.

(4) Thierfelder, L., Watkins, H., MacRae, C., Lamas, R., McKenna, W., Vosberg, H.-P., Seidman, J. G., and Seidman, C. E. (1994) α-Tropomyosin and cardiac troponin T mutations cause familial hypertrophic cardiomyopathy. *Cell 77*, 701−712.

(5) Nakajima-Taniguchi, C., Matsui, H., Nagata, S., Kishimoto, T., and Yamauchi-Takihara, K. (1995) Novel missense mutation in α-tropomyosin gene found in Japanese patients with hypertrophic cardiomyopathy. *J. Mol. Cell. Cardiol. 27*, 2053−2058.

(6) Bottinelli, R., Coviello, D. A., Redwood, C. S., Pellegrino, M. A., Maron, B. J., Spirito, P., Watkins, H., and Reggiani, C. (1998) A mutant tropomyosin that causes hypertrophic cardiomyopathy is expressed in vivo and associated with an increased calcium sensitivity. *Circ. Res. 82*, 106−115.

(7) Bai, F., Weis, A., Takeda, A. K., Chase, P. B., and Kawai, M. (2011) Enhanced active cross-bridges during diastole: Molecular pathogenesis of tropomyosin's HCM mutations. *Biophys. J. 100*, 1014−1023.

(8) Bing, W., Knott, A., Redwood, C., Esposito, G., Purcell, I., Watkins, H., and Marston, S. (2000) Effect of hypertrophic cardiomyopathy mutations in human cardiac muscle α-tropomyosin (Asp175Asn and Glu180Gly) on the regulatory properties of human cardiac troponin determined by in vitro motility assay. *J. Mol. Cell. Cardiol. 32*, 1489−1498.

(9) Chang, A. N., Harada, K., Ackerman, M. J., and Potter, J. D. (2005) Functional consequences of hypertrophic and dilated cardiomyopathy-causing mutations in α-tropomyosin. *J. Biol. Chem. 280*, 34343−34349.

(10) Prabhakar, R., Petrashevskaya, N., Schwartz, A., Aronow, B., Boivin, G. P., Molkentin, J. D., and Wieczorek, D. F. (2003) A mouse model of familial hypertrophic cardiomyopathy caused by an α-tropomyosin mutation. *Mol. Cell. Biochem. 251*, 33−42.

(11) Boussouf, S. E., Maytum, R., Jaquet, K., and Geeves, M. A. (2007) Role of tropomyosin isoforms in the calcium sensitivity of striated muscle thin filaments. *J. Muscle Res. Cell Motil. 28*, 49−58.

(12) Golitsina, N., An, Y., Greenfield, N. J., Thierfelder, L., Iizuka, K., Seidman, J. G., Seidman, C. E., Lehrer, S. S., and Hitchcock-DeGregori, S. E. (1997) Effects of two familial hypertrophic cardiomyopathy-causing mutations on α-tropomyosin structure and function. *Biochemistry 36*, 4637−4642.

(13) Golitsina, N., An, Y., Greenfield, N. J., Thierfelder, L., Iizuka, K., Seidman, J. G., Seidman, C. E., Lehrer, S. S., and Hitchcock-DeGregori, S. E. (1999) Effects of two familial hypertrophic cardiomyopathy-causing mutations on α-tropomyosin structure and function. *Biochemistry 38*, 3850.

(14) Kremneva, E., Boussouf, S., Nikolaeva, O., Maytum, R., Geeves, M. A., and Levitsky, D. I. (2004) Effects of two familial hypertrophic cardiomyopathy mutations in α-tropomyosin, Asp175Asn and Glu180Gly, on the thermal unfolding of actin-bound tropomyosin. *Biophys. J. 87*, 3922−3933.

(15) McLachlan, A. D., and Stewart, M. (1975) Tm Coiled-coil Interactions: Evidence for an Unstaggered Structure. *J. Mol. Biol. 98*, 293−304.

(16) McKillop, D. F. A., and Geeves, M. A. (1993) Regulation of the interaction between actin and myosin subfragment 1: Evidence for three states of the thin filament. *Biophys. J. 65*, 693−701.

(17) Vibert, P., Craig, R., and Lehman, W. (1997) Steric-model for activation of muscle thin filaments. *J. Mol. Biol. 266*, 8−14.

(18) Lehrer, S. S. (2011) The 3-state model of muscle regulation revisited: Is a fourth state involved? *J. Muscle Res. Cell Motil. 32*, 203−208.

(19) Moss, R. L., Razumova, M., and Fitzsimons, D. P. (2004) Myosin crossbridge activation of cardiac thin filaments: Implications for myocardial function in health and disease. *Circ. Res. 94*, 1290−1300.

(20) Sumida, J. P., Wu, E., and Lehrer, S. S. (2008) Conserved Asp-137 imparts flexibility to tropomyosin and affects function. *J. Biol. Chem. 283*, 6728−6734.

(21) Spudich, J., and Watt, S. (1971) The regulation of rabbit skeletal muscle contraction. I. Biochemical studies of the interaction of the tropomyosin-troponin complex with actin and the proteolytic fragments of myosin. *J. Biol. Chem. 246*, 4866−4871.

(22) Margossian, S., and Lowey, S. (1982) Preparation of myosin and its subfragments. *Methods Enzymol. 85*, 55−71.

(23) Van Eerd, J., and Kawasaki, Y. (1973) Effect of calcium on the interaction between subunits of troponin and tropomyosin. *Biochemistry 12*, 4972−4980.

(24) Sumida, J. P., Hayes, D., Langsetmo, K., and Lehrer, S. S. (2006) Tropomyosin: Charge effects in the hydrophobic ridge. *Biophys. J. 90* (Suppl.), 923a.

(25) Pato, M. D., Mak, A. S., and Smillie, L. B. (1981) Fragments of rabbit striated muscle α-tropomyosin. I. Preparation and characterization. *J. Biol. Chem. 256*, 593−601.

(26) Woods, E. F. (1977) Stability of segments of rabbit α-tropomyosin. *Aust. J. Biol. Sci. 30*, 527−542.

(27) Park, C., and Marqusee, S. (2004) Probing the high energy states by proteolysis. *J. Mol. Biol. 343*, 1467−1476.

(28) Nevzorov, I. A., Nikolaeva, O. P., Kainov, Y. A., Redwood, C. S., and Levitsky, D. I. (2011) Conserved noncanonical residue Gly-126 confers instability to the middle part of the tropomyosin molecule. *J. Biol. Chem. 286*, 15766−15772.
(29) Lehrer, S. S. (1978) Effects of an interchain disulfide bond on tropomyosin structure: Intrinsic fluorescence and circular dichroism studies. *J. Mol. Biol. 118*, 209−226.
(30) Ueno, H. (1984) Local structural changes in tropomyosin detected by a trypsin-probe method. *Biochemistry 23*, 4791−4798.
(31) Betteridge, D. R., and Lehrer, S. S. (1983) Two conformational states of didansylcystine-labeled rabbit cardiac tropomyosin. *J. Mol. Biol. 167*, 481−496.
(32) Ishii, Y., Hitchcock-DeGregori, S., Mabuchi, K., and Lehrer, S. S. (1992) Unfolding domains of recombinant fusion $\alpha\alpha$-tropomyosin. *Protein Sci. 1*, 1319−1325.
(33) Ishii, Y. (1994) The local and global unfolding of coiled-coil tropomyosin. *Eur. J. Biochem. 221*, 705−712.
(34) Phillips, G. N., Jr., Fillers, J. P., and Cohen, C. (1986) Tropomyosin crystal structure and muscle regulation. *J. Mol. Biol. 192*, 111−131.
(35) Hitchcock-DeGregori, S., and Varnell, T. (1990) Tropomyosin has discrete actin-binding sites with sevenfold and fourteen-fold periodicity. *J. Mol. Biol. 214*, 885−890.
(36) Mudalige, A. W., and Lehrer, S. S. (2010) What Region of Tropomyosin Interacts with the N-terminal Half of Troponin T? *Biophys. J. 98*, 351a.
(37) Geeves, M., Griffiths, H., Mijailovich, S., and Smith, D. (2011) Cooperative [Ca^{2+}]-dependent regulation of the rate of myosin binding to actin: Solution data and the tropomyosin chain model. *Biophys. J. 100*, 2679−2687.
(38) Loong, C. K., Zhou, H. X., and Chase, P. B. (2012) Persistence Length of Human Cardiac α-Tropomyosin Measured by Single Molecule Direct Probe Microscopy. *PLoS One 7*, e39676.
(39) Li, X. E., Holmes, K. C., Lehman, W., Jung, H., and Fischer, S. (2009) The shape and flexibility of tropomyosin coiled coils: Implications for actin filament assembly and regulation. *J. Mol. Biol. 395*, 327−339.
(40) Geeves, M. A., and Lehrer, S. S. (1994) Dynamics of the muscle thin filament regulatory switch: The size of the cooperative unit. *Biophys. J. 67*, 273−282.
(41) Maytum, R., Konrad, M., Lehrer, S. S., and Geeves, M. A. (2001) Regulatory properties of tropomyosin effects of length, isoform, and N-terminal sequence. *Biochemistry 40*, 7334−7341.
(42) Li, X. E., Lehman, W., Fischer, S., and Holmes, K. C. (2009) Curvature variation along the tropomyosin molecule. *J. Struct. Biol. 170*, 307−312.
(43) Minakata, S., Maeda, K., Oda, N., Wakabayashi, K., Nitanai, Y., and Maeda, Y. (2008) Two-crystal structures of tropomyosin C-terminal fragment 176−273: Exposure of the hydrophobic core to the solvent destabilizes the tropomyosin molecule. *Biophys. J. 95*, 710−719.
(44) Gibbons, I. R., Garbarino, J. E., Tan, C. E., Reck-Peterson, S. L., Vale, R. D., and Carter, A. P. (2005) The affinity of the dynein microtubule-binding domain is modulated by the conformation of its coiled-coil stalk. *J. Biol. Chem. 280*, 23960−23965.
(45) Kon, T., Imamula, K., Roberts, A. J., Ohkura, R., Knight, P. J., Gibbons, I. R., Burgess, S. A., and Sutoh, K. (2009) Helix sliding in the stalk coiled coil of dynein couples ATPase and microtubule binding. *Nat. Struct. Mol. Biol. 16*, 325−333.
(46) Croasdale, R., Ivins, F. J., Muskett, F., Daviter, T., Scott, D. J., Hardy, T., Smerdon, S. J., Fry, A. M., and Pfuhl, M. (2011) An undecided coiled coil: The leucine zipper of Nek2 kinase exhibits atypical conformational exchange dynamics. *J. Biol. Chem. 286*, 27537−27547.
(47) Kittel, C. (2004) *Solid State Physics*, Wiley, New York.
(48) Ishii, Y., and Lehrer, S. S. (1986) Effects of Troponin in the Conformation of Pyrene-Tropomyosin. *Biophys. J. 49*, 258a.
(49) Zhou, X., Morris, E. P., and Lehrer, S. S. (1995) Troponin I and troponin I-C binding to actin-tropomyosin and dissociation by myosin S1. *Biophys. J. 68*, A167.
(50) Mudalige, W. A., Tao, T. C., and Lehrer, S. S. (2009) Ca^{2+}-dependent photocrosslinking of tropomyosin residue 146 to residues 157−163 in the C-terminal domain of troponin I in reconstituted skeletal muscle thin filaments. *J. Mol. Biol. 389*, 575−583.
(51) Potter, J. D., and Gergely, J. (1974) Troponin, tropomyosin and actin interactions in the regulation of muscle contraction. *Biochemistry 13*, 2697−2703.
(52) Wang, C. K., and Cheung, H. C. (1985) Energetics of the binding of calcium and troponin I to troponin C from rabbit skeletal muscle. *Biophys. J. 48*, 727−739.
(53) Liao, R., Wang, C. K., and Cheung, H. C. (1994) Coupling of calcium to the interaction of troponin I with troponin C from cardiac muscle. *Biochemistry 33*, 12729−12734.
(54) Rysev, N. A., Karpicheva, O. E., Redwood, C. S., and Borovikov, Y. S. (2012) The effect of the Asp175Asn and Glu180Gly TPM1 mutations on actin-myosin interaction during the ATPase cycle. *Biochim. Biophys. Acta 1824*, 366−373.
(55) Hoffman, P. A., and Fuchs, F. (1987) Effect of length and cross-bridge attachment on Ca^{2+} binding to cardiac troponin C. *Am. J. Physiol. 253*, C90−C96.
(56) Stelzer, J. E., Larsson, L., Fitzsimons, D. P., and Moss, R. L. (2006) Activation dependence of stretch activation in mouse skinned myocardium: Implications for ventricular function. *J. Gen. Physiol. 127*, 95−107.
(57) Bullard, B., and Pastore, A. (2011) Regulating the contraction of insect flight muscle. *J. Muscle Res. Cell Motil. 32*, 303−313.